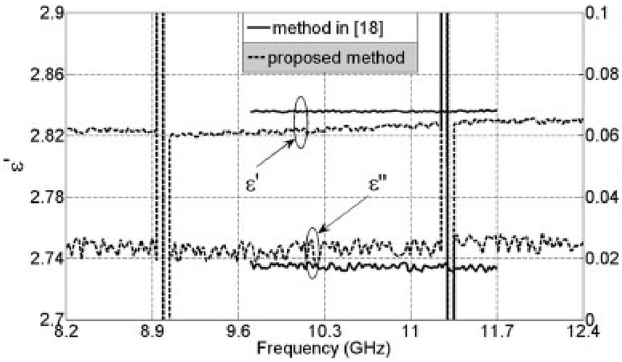

Figure 3 Measured permittivity of a polyvinyl-chloride (PVC) sample (20 mm) by the proposed method and that in Ref. 18

the method may produce singularity points in the extracted complex permittivity. The method is validated by calibrated and uncalibrated complex S-parameter measurements of a PVC sample.

ACKNOWLEDGMENTS

U.C. Hasar (Mehmetcik) would like to thank TUBITAK (The Scientific and Technological Research Council of Turkey) Münir Birsel National Doctorate Scholarship and YOK (The Higher Education Council of Turkey) Doctorate Scholarship for supporting his studies.

REFERENCES

1. R. Zoughi, Microwave non-destructive testing and evaluation, Kluwer Academic Publishers, The Netherlands, 2000.
2. L.F. Chen, C.K. Ong, C.P. Neo, V.V. Varadan, and V.K. Varadan, Microwave electronics: Measurement and materials characterization, Wiley, New York, 2004.
3. M.N. Afsar, J.R. Birch, and R.N. Clarke, The measurement of the properties of materials, Proc IEEE 74 (1986), 183–199.
4. J. Baker-Jarvis, R.G. Geyer, J.H. Grosvenor, M.D. Jones, B. Riddle, C.M. Weil, and J. Krupka, Dielectric characterization of low-loss materials: A comparison of techniques, IEEE Trans Dielectr Electr Insul 5 (1998), 571–577.
5. J. Baker-Jarvis, Transmission/reflection and short-circuit line permittivity measurements, National Institute Standards and Technology, Boulder, CO, 1990,Technical Note 1341.
6. A.M. Nicolson and G. Ross, Measurement of the intrinsic properties of materials by time-domain techniques, IEEE Trans Instrum Meas 19 (1970), 377–382.
7. W.B. Weir, Automatic measurement of complex dielectric constant and permeability at microwave frequencies, Proc IEEE 62 (1974), 33–36.
8. E. Nyfors, Industrial microwave sensors—A review, Subsurface Sensing Technol Appl 1 (2000), 23–43.
9. M.Q. Lee and S. Nam, An accurate broadband measurement of substrate dielectric constant, IEEE Microwave Guided Wave Lett 6 (1996), 168–170.
10. M.D. Janezic and J.A. Jargon, Complex permittivity determination from propagation constant measurements, IEEE Microwave Guided Wave Lett 9 (1999), 76–78.
11. I. Huynen, C. Steukers, and F. Duhamel, A wideband line-line dielectrometric method for liquids, soils, and planar substrates, IEEE Trans Instrum Meas 50 (2001), 1343–1348.
12. K.-H. Baek, H.-Y. Sung, and W.S. Park, A 3-position transmission/reflection method for measuring the permittivity of low loss materials, IEEE Microwave Guided Wave Lett 5 (1995), 3–5.
13. C. Wan, B. Nauwelaers, W. De Raedt, and M. Van Rossum, Complex permittivity measurement method based on asymmetry of reciprocal two-ports, Electron Lett 32 (1996), 1497.
14. U.C. Hasar, Calibration-independent method for complex permittivity determination of liquid and granular materials, Electron Lett 44 (2008), 585–587.
15. U.C. Hasar, A new calibration-independent method for complex permittivity extraction of solid dielectric materials, IEEE Microwave Wireless Compon Lett, in press.
16. G.F. Engen and C.A. Hoer, 'Thru-Reflect-Line': An improved technique for calibrating the dual six-port automatic network analyzer, IEEE Trans Microwave Theory Tech 27 (1979), 987–993.
17. U.C. Hasar, A self-checking technique for materials characterization using calibration-independent measurements of reflecting lines, Microwave Opt Technol Lett, in press.
18. U.C. Hasar, Two novel amplitude-only methods for complex permittivity determination of medium- and low-loss materials, Meas Sci Technol 19 (2008), 055706-055715.
19. C. Wan, B. Nauwelaers, W. De Raedt, and M. Van Rossum, Two new measurement methods for explicit determination of complex permittivity, IEEE Trans Microwave Theory Tech 46 (1998), 1614–1619.

HEARING AID-COMPATIBLE INTERNAL PENTA-BAND ANTENNA FOR CLAMSHELL MOBILE PHONE

Kin-Lu Wong and Ming-Fang Tu
Department of Electrical Engineering, National Sun Yat-Sen University, Kaohsiung 804, Taiwan; Corresponding author: tumf@ema.ee.nsysu.edu.tw

Received 29 September 2008

ABSTRACT: *This article presents a promising internal penta-band antenna for the clamshell mobile phone to meet the hearing aid compatibility (HAC) standard ANSI C63.19-2006. The antenna is an ultra-wideband (UWB) coupled-fed loop antenna to be mounted at the hinge of the clamshell mobile phone. Over the five operating bands of GSM850/900/1800/1900/UMTS covered by the antenna, the near-field distributions and their E-field and H-field strengths on the 50 × 50 mm² reference plane centered 10 mm above the center of the acoustic output of the mobile phone are evaluated. From the obtained near-field strengths, all the five operating bands fall into the M3 or M4 category, making the mobile phone with the studied internal antenna as a hearing aid-compatible wireless device. Effects of various groundplane lengths of the mobile phone on the HAC results are also analyzed. In addition, the mobile phone with the studied internal antenna also meets the specific absorption rate (SAR) limit of 1.6 W/kg for the 1 g head tissue or 2.0 W/kg for the 10 g head tissue.* © 2009 Wiley Periodicals, Inc. Microwave Opt Technol Lett 51: 1408–1413, 2009; Published online in Wiley InterScience (www.interscience.wiley.com). DOI 10.1002/mop.24353

Key words: *internal mobile phone antennas; penta-band antennas; clamshell mobile phones; hearing aid compatibility (HAC); specific absorption rate (SAR)*

1. INTRODUCTION

The hearing aid compatibility (HAC) standard, developed in 2001 and updated in 2006, requires that at least half of all mobile phones on the market of the U.S. must have RF interference level of category M3 or M4 of ANSI C63.19-2006 [1]. It is also noted that although there have been some studies on the HAC problem of the mobile phone with a hearing aid [2–4], practical solutions of the promising internal mobile phone antenna capable of GSM850/900/1800/1900/UMTS penta-band operation and satisfying the HAC standard [1] are still not available in the published articles.

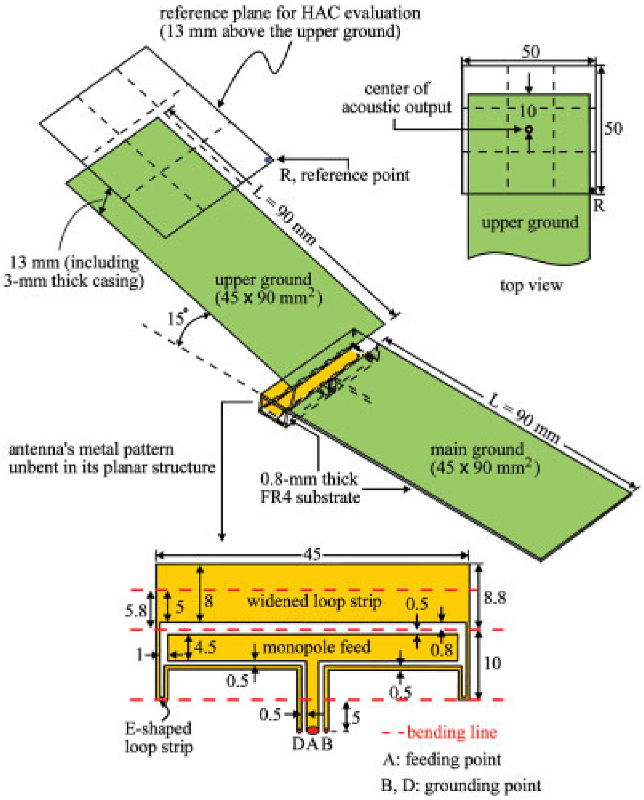

Figure 1 HAC simulation model of the clamshell mobile phone with the studied penta-band internal antenna. [Color figure can be viewed in the online issue, which is available at www.interscience.wiley.com]

Here, in this article we present the study on an HAC penta-band internal mobile phone antenna. The studied antenna is an ultra-wideband (UWB) coupled-fed loop antenna suitable to be mounted at the hinge of the clamshell mobile phone, and its return loss, input impedance, and far-field radiation characteristics have been presented and discussed in [5]. The present article reports an extension of the previous work. By using the HAC simulation model provided by SPEAG SEMCAD [6], the near-field radiation characteristics including the near-field distributions and the electric near-field (E-field) and magnetic near-field (H-field) strengths are evaluated to determine the HAC category of the studied antenna. It is required to be in category M3 or M4 for the tested antenna to meet the HAC standard specified in ANSI C63.19-2006 [1]. Largely owing to its UWB property, which implies a low-Q characteristic [4], the studied antenna can meet the required HAC standard. Details of the HAC simulation model and results are presented in this article. Further, the specific absorption rate (SAR) of the head tissue in 1 g and 10 g from exposure to the radiation of the studied antenna is also found from simulation using SPEAG SEMCAD [6] to meet the limit of 1.6 W/kg and 2.0 W/kg, respectively. Because the SAR is also an important near-field characteristic of the mobile phone antenna and is required for the practical mobile phone applications [7–10], the obtained SAR results of the studied antenna are also presented.

2. HAC RESULTS OF THE STUDIED ANTENNA

Figure 1 shows the HAC simulation model of the clamshell mobile phone with the studied penta-band internal antenna. The studied antenna is a coupled-fed loop antenna with a small volume of $5.8 \times 10 \times 45$ mm^3 or 2.6 cm^3 only. Its detailed design dimensions and far-field radiation characteristics have been presented in

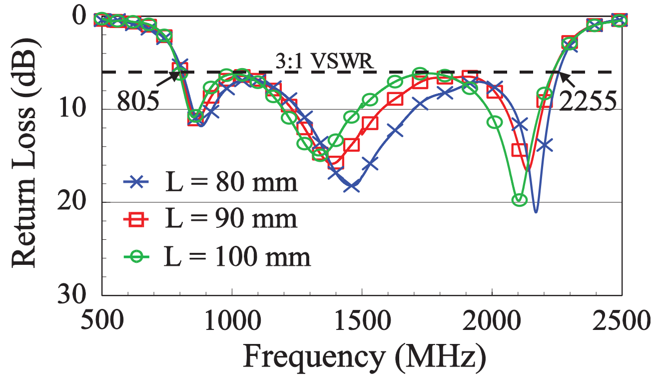

Figure 2 Simulated return loss for the studied antenna with various groundplane lengths. [Color figure can be viewed in the online issue, which is available at www.interscience.wiley.com]

[5]. On the basis of the standard ANSI C63.19-2006 [1], the HAC results should be evaluated on the 50×50 mm^2 reference plane centered 10 mm above the center of the acoustic output in the mobile phone casing. For the studied clamshell mobile phone, the acoustic output is located along the centerline of the mobile phone and is with a distance of 10 mm to the top edge of the upper ground. By assuming a 3 mm thickness between the mobile phone

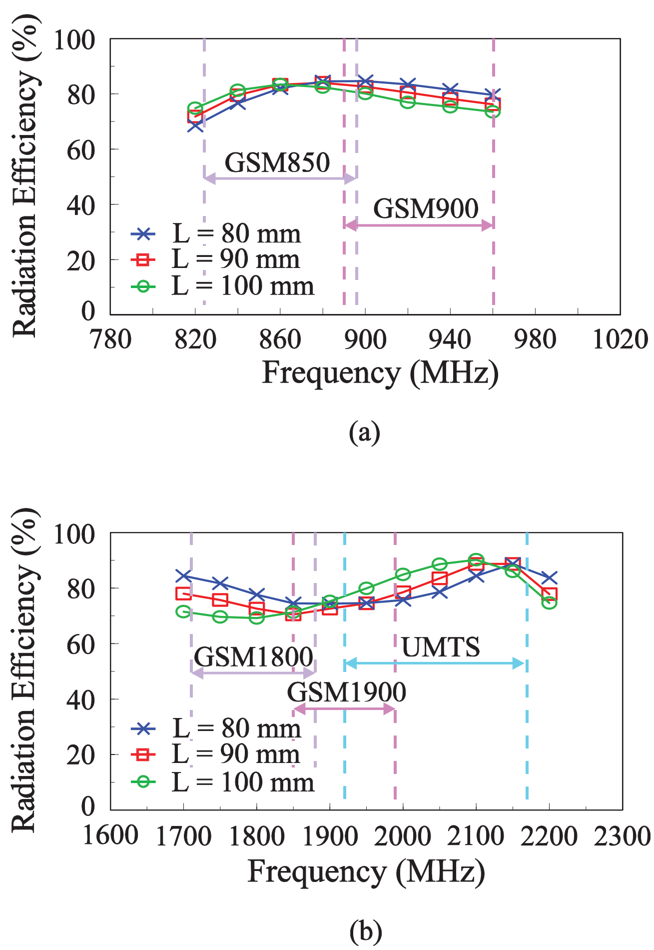

Figure 3 Simulated radiation efficiency for the studied antenna with various groundplane lengths. (a) GSM850/900 bands. (b) GSM1800/1900/UMTS bands. [Color figure can be viewed in the online issue, which is available at www.interscience.wiley.com]

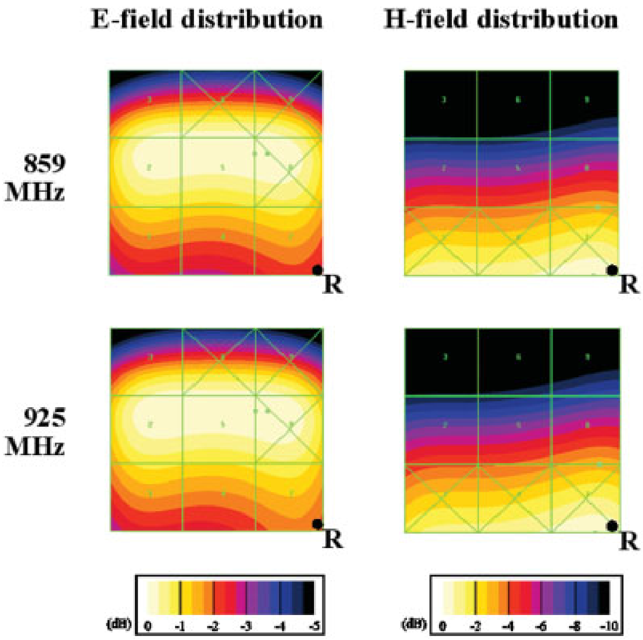

Figure 4 Simulated near-field (E-field and H-field) distributions at 859 and 925 MHz on the reference plane for the studied antenna with $L = 90$ mm; point R is the reference point as indicated in Figure 1. [Color figure can be viewed in the online issue, which is available at www.interscience.wiley.com]

casing and the upper ground, the reference plane for HAC evaluation is set at 13 mm above the upper ground; that is, the reference plane is 10 mm above the mobile phone casing. Also note that the reference plane is divided into nine equal cells, and following the rating methodology of the ANSI C63.19-2006 [1], the E-field and H-field strengths are determined by excluding three consecutive cells along the boundary of the reference plane that have the strongest field strengths [see the three crossed cells in each near-field distribution shown in Figures 4 and 5, which will be discussed later].

To begin with the study, the simulated return loss of the antenna with the groundplane lengths varied from 80 to 100 mm is shown in Figure 2. Note that both the main ground and upper ground are of the same length L, and the antenna is mounted at the hinge of the clamshell mobile phone. Other dimensions are the same as given in Figure 1. The studied antenna shows stable UWB behavior from about 805 to 2255 GHz (3:1 VSWR) for various promising groundplane lengths. The small variations in the obtained UWB bandwidth of 1450 MHz, especially showing almost no variations in the lower-edge frequency at about 805 MHz, are the advantageous feature of the loop antenna [10–14] over the traditional mobile phone antennas such as the internal PIFAs [15].

From the results in Figure 2, there are three resonant modes excited for the antenna. The first resonant mode occurs at about 900 MHz and is the 0.5 wavelength loop resonant mode contributed by the E-shaped loop strip; the second one occurs at about 1400 MHz and is mainly controlled by the two grounds (main and upper grounds) of the mobile phone; the third one occurs at about 2100 MHz and is the 0.25-wavelength resonant mode generated by the monopole feed [5]. The UWB bandwidth formed by the three resonant modes easily covers GSM850 (824–894 MHz), GSM900 (890–960 MHz), GSM1800 (1710–1880 MHz), GSM1900 (1850–1990 MHz), and UMTS (1920–2170 MHz) for wireless wide area network (WWAN) penta-band operation.

The simulated radiation efficiency for frequencies over the five operating bands of the studied antenna with the groundplane length L varied from 80 to 100 mm is shown in Figure 3. In Figure 3(a), results for the GSM850/900 bands are presented, and small variations in the radiation efficiency owing to the length variations of the ground plane are seen. For the results over the GSM1800/1900/UMTS bands shown in Figure 3(b), similar small variations are also seen. Over the five operating bands, the radiation efficiency is all better than 65%.

After ensuring good impedance matching and radiation characteristics for the studied antenna with various promising groundplane lengths, the HAC results are studied. Figure 4 shows the simulated near-field distributions at 859 and 925 MHz (central frequencies of the GSM850 and GSM900 bands) on the reference plane for the antenna with $L = 90$ mm, whereas the corresponding near-field distributions at 1795, 1920, and 2045 MHz (central frequencies of the GSM1800, GSM1900, and UMTS bands) are shown in Figure 5. In the study, the delivered power is 33 dBm (2 W continuous wave power) at 859 and 925 MHz, and is 30 dBm (1 W continuous wave power) at 1795, 1920, and 2045 MHz. Note that there are three consecutive crossed cells along the boundary of the reference plane, which are excluded from the near-field strength evaluation.

For the H-field distributions in Figures 4 and 5 and the E-field distributions in Figure 5, the maximum field distribution is seen to be on the eight cells along the boundary of the reference plane.

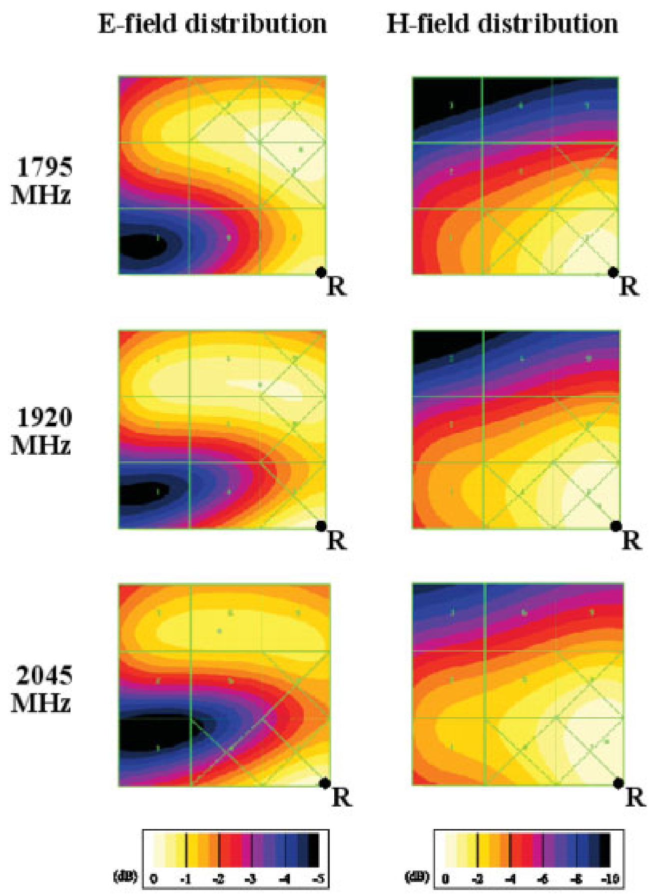

Figure 5 Simulated near-field (E-field and H-field) distributions at 1795, 1920, and 2045 MHz on the reference plane for the studied antenna with $L = 90$ mm; point R is the reference point as indicated in Figure 1. [Color figure can be viewed in the online issue, which is available at www.interscience.wiley.com]

M3 or M4 rating for the E-field and H-field is obtained, the mobile phone with the studied antenna at 859 and 925 MHz can be rated as category M3. With this rating, the mobile phone can be rated as a hearing aid-compatible wireless device for operating at 859 and 925 MHz [1, 4].

The simulated near-field strengths at 1795, 1920, and 2045 MHz for the antenna with L = 80, 90, and 100 mm are shown in Figure 7. Note that for frequencies at 1795 and 1920 MHz, the strength level of each category is 10 dB lower than that of the same category at 859 and 925 MHz [1]. Also, the strength level of each category at 2045 MHz (UMTS system) is 2.5 dB higher than that of the same category at 1795 and 1920 MHz (GSM system) [1]. Following the same rating methodology discussed in Figure 6, the mobile phone with the studied antenna with various groundplane lengths is rated as category M3 for operating at 2045 MHz (UMTS system). Although at 1795 and 1920 MHz (GSM1800/1900 systems), however, results indicate that only for L = 80 and 90 mm, the mobile phone with the studied antenna is rated as category M3. For L = 100 mm, the mobile phone with the studied antenna is rated as category M2 only. However, considering for the practical working phone condition in which lossy electronic elements such as the LCD display, battery, and so on are present, the obtained near-field emission of the mobile phone could be decreased. It is hence very possible that the clamshell mobile phone with the studied antenna can meet the M3 rating at 2045 MHz for L = 100

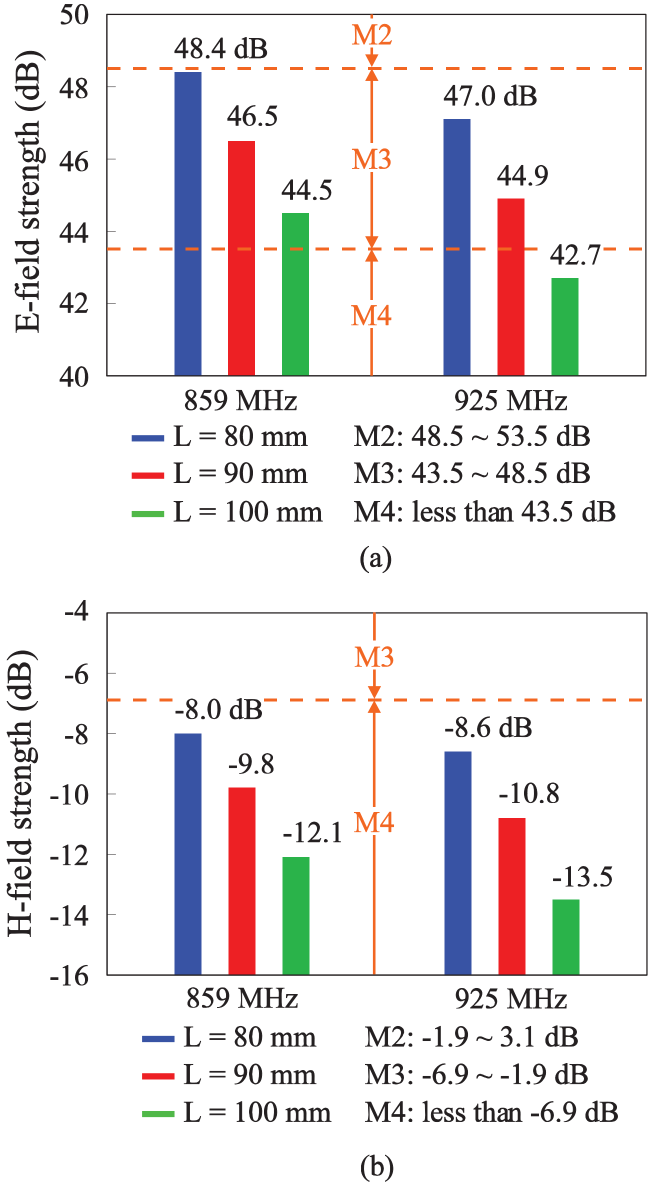

Figure 6 Simulated near-field strengths at 859 and 925 MHz on the reference plane for the studied antenna with L = 80, 90, and 100 mm. (a) E-field strength. (b) H-field strength. [Color figure can be viewed in the online issue, which is available at www.interscience.wiley.com]

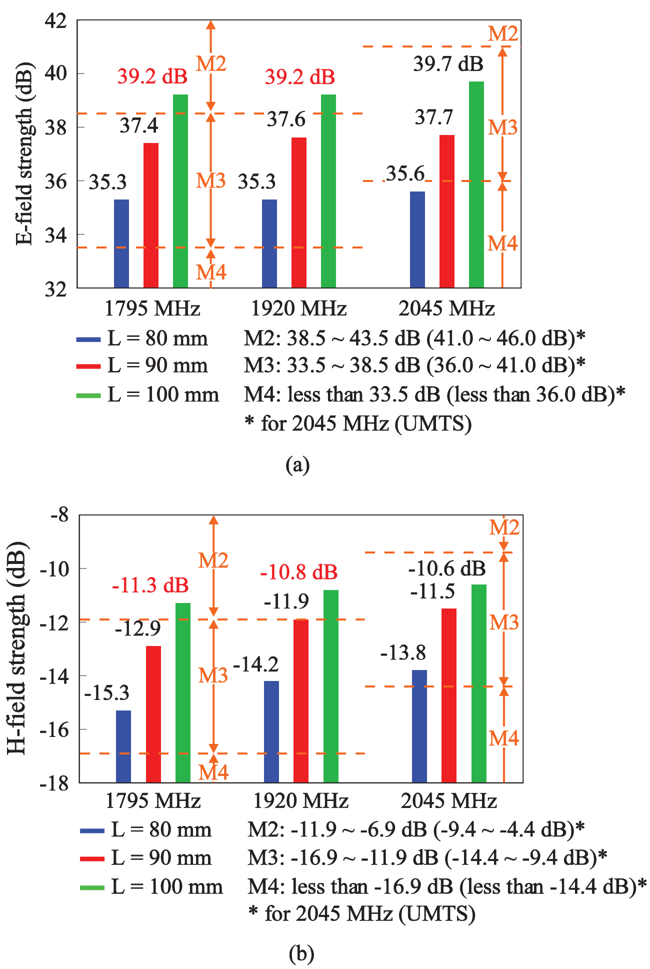

Figure 7 Simulated near-field strengths at 1795, 1920, and 2045 MHz on the reference plane for the studied antenna with L = 80, 90, and 100 mm. (a) E-field strength. (b) H-field strength. [Color figure can be viewed in the online issue, which is available at www.interscience.wiley.com]

That is, the maximum field distribution is not at the center of the reference plane or at the center of the acoustic output. By following the HAC rating methodology [1], such maximum field distributions can be excluded from near-field strength evaluation, and thus, a lower HAC category rating can be obtained. For the E-field distribution seen in Figure 4, however, the maximum field distribution locates at the center of the reference plane. In this case, the HAC category rating could be higher owing to the relatively strong E-field distribution at 859 and 925 MHz.

Figure 6 shows the simulated near-field strengths at 859 and 925 MHz (GSM850/900 systems) for the antenna with L = 80, 90, and 100 mm. The strength range for each category according to the standard ANSI C63.19-2006 [1] is also given in the figure. For the E-field strength, it falls in category M3, except for L = 100 mm in which the E-field strength even falls in category M4. For the H-field strength, as seen in the field distributions in Figure 4, it falls in category M4. Because either

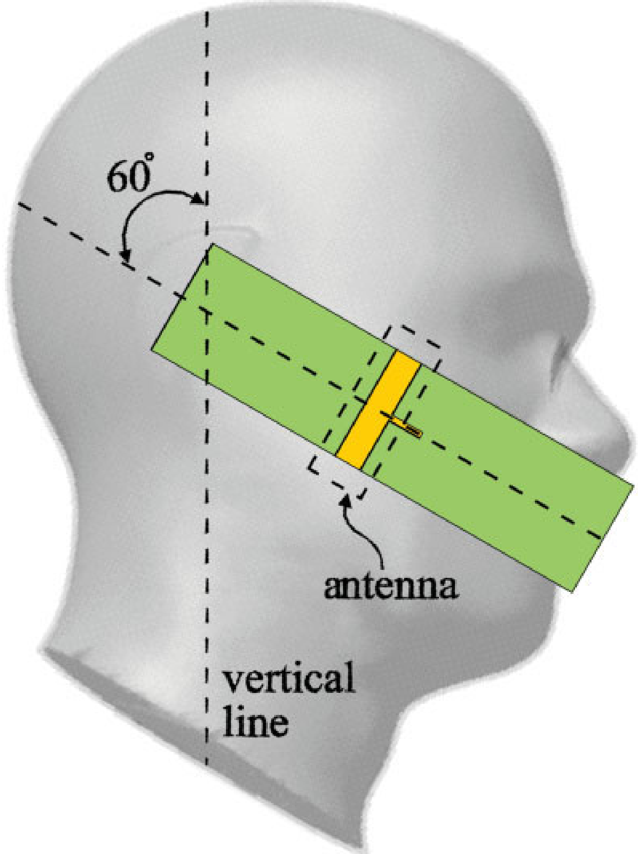

Figure 8 SAR simulation model of the clamshell mobile phone with the studied antenna. [Color figure can be viewed in the online issue, which is available at www.interscience.wiley.com]

mm. From the obtained results, the studied mobile phone with various promising groundplane lengths can be rated as a hearing aid-compatible wireless device for GSM850/900/1800/1900/UMTS systems.

It is also noted that the groundplane effect on the near-field strengths observed at higher frequencies in Figure 7 is different from that at lower frequencies in Figure 6. The field strengths for both the E-field and H-field at 1795, 1925, and 2045 MHz are seen to increase with increasing groundplane length L, whereas the field strengths at 895 and 925 MHz are decreased with increasing groundplane length L. This is largely owing to the different groundplane lengths in terms of the operating wavelength at lower and higher frequencies.

3. SAR RESULTS OF THE STUDIED ANTENNA

The SAR study of the clamshell mobile phone is also studied. The SAR results for the case of $L = 90$ mm are analyzed, and the SAR simulation model with the top portion of the upper ground of the clamshell mobile phone attached onto the head phantom is shown in Figure 8. The simulated head phantom is provided by SPEAG SEMCAD [6]. The centerline of the mobile phone is oriented with an angle of 60° to the vertical line in the study, and the top portion of the upper ground is spaced with a small distance of 4 mm away from the ear position of the head phantom. Before evaluating the SAR results, the impedance matching of the studied antenna with and without the head phantom is first verified. Small variations in the impedance matching over the obtained UWB bandwidth are seen, and the impedance matching of the five tested frequencies

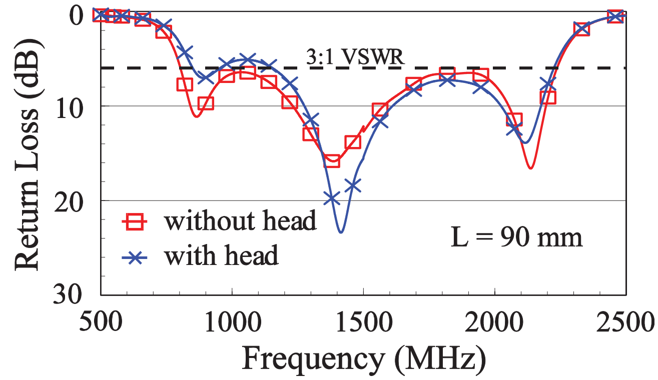

Figure 9 Simulated return loss of the studied antenna with and without the head phantom. [Color figure can be viewed in the online issue, which is available at www.interscience.wiley.com]

remains better than 6-dB return loss (Figure 9). This behavior is similar to that observed for the case when the user's hand holds the mobile phone at the position without enclosing the embedded antenna [16–19]. However, it should be noted that the radiation efficiency of the antenna will be greatly decreased by at least 3 dB because of the presence of the head phantom or the user's head, which is a very lossy material and will effectively absorb a large portion of the antenna's radiated wave power.

At 859 and 925 MHz, the SAR is tested using 24 dBm, whereas at 1795, 1920, and 2045 MHz, the SAR is tested using 21 dBm (considering a user channel being 1/8 of a time slot at lower and higher frequencies). The obtained SAR results in 1 g and 10 g of head tissue from exposure to the antenna radiation are listed in Table 1 for comparison. The corresponding simulated 1 g SAR distributions at 859, 925, 1795, 1920, and 2045 MHz for the studied antenna with $L = 90$ mm are shown in Figure 10. In the figure, the square marks represent the SAR maximum at each frequency. For all the five frequencies, the SAR maximum is all located at about the cheek position of the head phantom or close to the hinge position of the mobile phone. This is reasonable since the antenna is located at the hinge position. From the obtained results, both the 1 g and 10 g SAR results at all frequencies meet the SAR limit of 1.6 W/kg and 2.0 W/kg, respectively.

4. CONCLUSION

The HAC and SAR results of an UWB coupled-fed loop antenna for application in the clamshell phone have been studied. The HAC and SAR simulation models provided by SEMCAD are adopted in this study. The antenna shows a 3:1 VSWR UWB bandwidth of about 1.45 GHz (from 805 to 2255 MHz), allowing it to easily cover GSM850/900/1800/1900/UMTS operation. With penta-band operation obtained, the excited near-field strengths of the antenna

TABLE 1 Simulated SAR in 1 g and 10 g of Head Tissue from Exposure to Radiation of the Studied Antenna with L = 90 mm

Frequency (MHz)	1 g SAR (W/kg)	10 g SAR (W/kg)
859	1.39	0.94
925	1.43	0.97
1795	0.9	0.53
1920	1.05	0.62
2045	1.16	0.69

The upper ground is spaced 4 mm away from the head phantom.

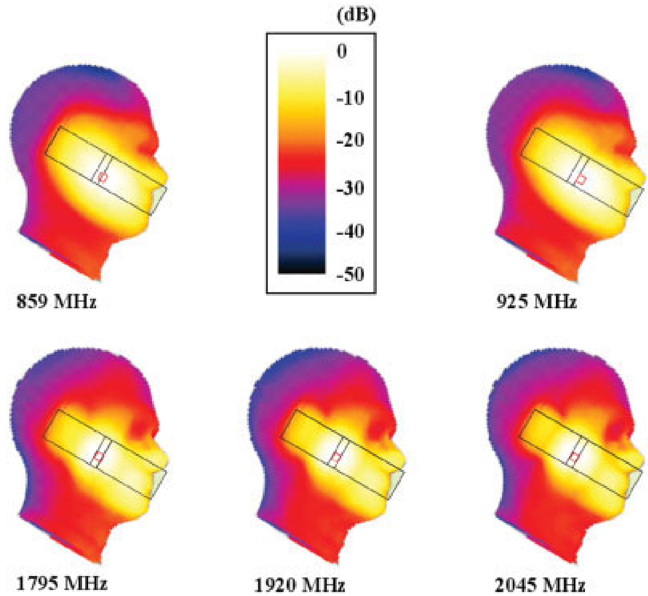

Figure 10 Simulated 1 g SAR distributions at 859, 925, 1795, 1920, and 2045 MHz for the studied antenna with $L = 90$ mm. [Color figure can be viewed in the online issue, which is available at www.interscience.wiley.com]

have also been evaluated and rated to be in category M3 or M4. That is, the clamshell mobile phone with the studied antenna can be rated as a hearing aid-compatible wireless device. For the SAR evaluation, the obtained 1 g and 10 g SAR results of the studied clamshell mobile phone are also smaller than the SAR limit of 1.6 W/kg and 2.0 W/kg, respectively. The studied UWB antenna is hence a promising antenna solution for achieving penta-band WWAN operation and meeting the HAC requirement and SAR limit for practical applications in the clamshell mobile phone.

REFERENCES

1. American National Standard for Method of Measurement of Compatibility between Wireless Communication Devices and Hearing Aids (ANSI C63.19-2006), American National Standards Institute, New York, 2006.
2. M. Okoniewski and M.A. Stuchly, Modeling of interaction of electromagnetic fields from a cellular phone with hearing aids, IEEE Trans Microw Theory Tech 46 (1998), 1686–1693.
3. K. Caputa, N.A. Stuchly, M. Skopec, H.I. Bassen, P. Ruggera, and M. Kanda, Evaluation of electromagnetic interference from a cellular telephone with a hearing aid, IEEE Trans Microw Theory Tech 48 (2000), 2148–2154.
4. T. Yang, W.A. Davis, W.L. Stutzman, and M.C. Huynh, Cellular-phone and hearing-aid interaction: An antenna solution, IEEE Antenn Propag Mag 50 (2008), 51–65.
5. K.L. Wong and S.Y. Tu, Ultra-wideband coupled-fed loop antenna for penta-band folder-type mobile phone, Microwave Opt Technol Lett 50 (2008), 2706–2712.
6. Available at: http://www.semcad.com, SPEAG SEMCAD, Schmid & Partner Engineering AG.
7. O. Kivekas, J. Ollikainen, T. Lehtiniemi, and P. Vainikainen, Bandwidth, SAR, and efficiency of internal mobile phone antennas, IEEE Trans Electromagnetic Compatibility 46 (2004), 71–86.
8. Z. Li and Y. Rahmat-Samii, Optimization of PIFA-IFA combination in handset antenna design, IEEE Trans Antenn Propag 53 (2005), 1770–1777.
9. J.C. Lin, Specific absorption rates induced in head tissues by microwave radiation from cell phones, Microwave 40 (2001), 22–25.
10. Y.W. Chi and K.L. Wong, Internal compact dual-band printed loop antenna for mobile phone application, IEEE Trans Antenn Propag 55 (2007), 1457–1462.
11. C.H. Wu and K.L. Wong, Internal hybrid loop/monopole slot antenna for quad-band operation in the mobile phone, Microwave Opt Technol Lett 50 (2008), 795–801.
12. C.I. Lin and K.L. Wong, Internal multiband loop antenna for GSM/DCS/PCS/ UMTS operation in the small-size mobile phone, Microwave Opt Technol Lett 50 (2008), 1279–1285.
13. K.L. Wong and C.H. Huang, Printed loop antenna with a perpendicular feed for penta-band mobile phone application, IEEE Trans Antenn Propag 56 (2008), 2138–2141.
14. Y.W. Chi and K.L. Wong, Compact multiband folded loop chip antenna for small-size mobile phone, IEEE Trans Antenn Propag, in press.
15. K.L. Wong, Planar antennas for wireless communications, Wiley, New York, 2003.
16. C.M. Su, C.H. Wu, K.L. Wong, S.H. Yeh, and C.L. Tang, User's hand effects on EMC internal GSM/DCS dual-band mobile phone antenna, Microwave Opt Technol Lett 48 (2006), 1563–1569.
17. C.I. Lin and K.L. Wong, Internal meandered loop antenna for GSM/DCS/PCS multiband operation in a mobile phone with the user's hand, Microwave Opt Technol Lett 49 (2007), 759–765.
18. C.I. Lin and K.L. Wong, Printed monopole slot antenna for internal multiband mobile phone antenna, IEEE Trans Antenn Propag 55 (2007), 3690–3697.
19. C.H. Wu and K.L. Wong, Internal shorted planar monopole antenna embedded with a resonant spiral slot for penta-band mobile phone application, Microwave Opt Technol Lett 50 (2008), 529–536.

A SIMPLE SWITCHED BEAMFORMING NETWORK FOR FOUR-BEAM BUTLER MATRIX

Jae Hee Kim and Wee Sang Park
Department of EEE, Pohang University of Science and Technology, Pohang, Gyeongbuk, Republic of Korea; Corresponding author: jaehee@postech.ac.kr

Received 29 September 2008

ABSTRACT: *A simple switched beamforming network with one 90° hybrid, two switches, and delay lines is designed. By controlling the switches, the antenna can produce four beams with the phase differences between adjacent radiating elements being ±135° and ±45°. The proposed feed network is simple, provides a tapered amplitude distribution, and has the same phase characteristics as the four-beam Butler matrix feed network. The measured S11 of the proposed antenna is less than −10 dB at the operating frequency of 11.2 GHz. When switch 1 is in the "on" position and switch 2 is in the "off" position, or when both switches are in the "on" position, the measured radiation pattern shows that the scan angles are −12° and +35°. The proposed array antenna has the advantage of low cost, small volume, and easy fabrication.* © 2009 Wiley Periodicals, Inc. Microwave Opt Technol Lett 51: 1413–1416, 2009; Published online in Wiley InterScience (www.interscience.wiley.com). DOI 10.1002/mop.24352

Key words: *butler matrix; switched-beams; beamforming network; 90° hybrid; array antenna*

1. INTRODUCTION

A phased array antenna [1] is used to direct a signal in a given direction. The Butler matrix design [2] is widely used due to its simple design and its ability to form orthogonal beams. This design selects appropriate beams that have been constructed by a feed